

Supplemental Material for

Linking Structural Properties with Functionality in Solar Cell Materials – The Effective Mass and Effective Density of States

Thomas Kirchartz^{1,2} and Uwe Rau¹

¹IEK5-Photovoltaics, Forschungszentrum Jülich, 52425 Jülich, Germany

²Faculty of Engineering and CENIDE, University of Duisburg-Essen, Carl-Benz-Str. 199, 47057 Duisburg, Germany

Table I: Summary of the key relations for absorption and recombination that are of greatest importance for the main paper. The equations below are discussed in this supplemental material document in more detail.

quantity	Dependence on effective mass m_{eff}
absorption coefficient α_{dir} (direct semiconductor) ¹	$\alpha_{\text{dir}} = \frac{8.77 \times 10^4}{\text{cm} \sqrt{\text{eV}}} \frac{E_g (1 + m/m_{\text{eff}})}{E n_r} \left(\frac{m_{\text{eff}}}{m} \right)^{3/2} \sqrt{E - E_g}$
absorption coefficient α_{ind} (indirect semiconductor) ²	$\alpha_{\text{ind}} = \frac{\hbar}{3\pi} \alpha_{\text{fine}} a_H^2 \frac{R_H}{E} \varepsilon_{r,\text{opt}} n_r \frac{p_{\text{cv}}^2}{2m} \left(\frac{m_{\text{eff}}}{\hbar^2} \right)^3 \frac{M_{\text{val}} D_{ij}^2}{\rho \omega_{ij} (E_{g0} - E)}$ $\times \left[f_{\text{BE}}(\omega_{ij}) (E - E_g + \hbar \omega_{ij}) + (f_{\text{BE}}(\omega_{ij}) + 1) (E - E_g - \hbar \omega_{ij}) \right]$
Capture cross section (for multiphonon transitions) ³⁻⁵	$\sigma \propto \sqrt{\frac{m_{\text{eff}}}{4kT}} \frac{\pi}{\omega \hbar^2} \frac{ V_{nk} ^2}{\sqrt{p \sqrt{1+x^2}}}$ $\times \exp \left[p \left(\frac{\hbar \omega}{2kT} + \sqrt{1+x^2} - x \cosh \left(\frac{\hbar \omega}{2kT} \right) - \ln \left(\frac{1 + \sqrt{1+x^2}}{x} \right) \right) \right]$
Thermal velocity	$v_{\text{th}} = \sqrt{8kT/\pi m_{\text{eff}}}$
SRH lifetime (for multiphonon transitions)	$\tau = (\sigma v_{\text{th}} N_t)^{-1} = \text{const.}$

1. Absorption coefficients for parabolic bands

In the following, we will discuss the most important aspects of the tables in the main paper in more detail and provide equations without proportionality signs. We will use the symbols q for the elementary charge, kT for the thermal energy, m for the free electron mass ($m = 9.109 \times 10^{-31}$ kg), m_{eff} for the effective mass (in kg), \hbar for the reduced Planck's constant

($\hbar = 6.582 \times 10^{-16}$ eVs), n_r as the (real part of the) refractive index, E_g as the band gap of our semiconductor and E as the photon energy.

According to Ridley, the absorption coefficient α_{dir} for interband transitions in a direct band gap semiconductor is given by¹

$$\alpha_{\text{dir}} = \frac{2}{3} \alpha_{\text{fine}} a_H^2 \left(\frac{R_H}{E} \right) \frac{E_g (1 + m/m_{\text{eff}})}{n_r} \left(\frac{m_{\text{eff}}}{\hbar^2} \right)^{3/2} \sqrt{E - E_g} \quad (\text{S1})$$

where the dimensionless fine structure constant is defined as

$$\alpha_{\text{fine}} = \frac{q^2}{4\pi\epsilon_0\hbar c} = 7.297 \times 10^{-3}, \quad (\text{S2})$$

the Bohr radius

$$a_H = \frac{4\pi\epsilon_0\hbar^2}{mq^2} = 5.292 \times 10^{-11} \text{ m}, \quad (\text{S3})$$

and the Rydberg energy

$$R_H = \frac{q^2}{8\pi\epsilon_0 a_H} = 13.605 \text{ eV}. \quad (\text{S4})$$

It is useful to rewrite Eq. (S1) to obtain

$$\begin{aligned} \alpha_{\text{dir}} &= \frac{2}{3} \alpha_{\text{fine}} a_H^2 \left(\frac{R_H}{E} \right) \frac{E_g (1 + m/m_{\text{eff}}) m^{3/2}}{\hbar^3 n_r} \left(\frac{m_{\text{eff}}}{m} \right)^{3/2} \sqrt{E - E_g} \\ &= \alpha_{00} \frac{E_g (1 + m/m_{\text{eff}})}{E n_r} \left(\frac{m_{\text{eff}}}{m} \right)^{3/2} \sqrt{E - E_g} \end{aligned} \quad (\text{S5})$$

using a prefactor consisting only of natural constants

$$\begin{aligned} \alpha_{00} &= \frac{2}{3} \alpha_{\text{fine}} a_H^2 R_H \frac{m^{3/2}}{\hbar^3} \\ &= 8.77 \times 10^4 \text{ cm}^{-1} \text{ eV}^{-1/2} \end{aligned} \quad (\text{S6})$$

In case of an indirect semiconductor, we can write²

$$\begin{aligned} \alpha_{\text{ind}} &= \frac{\hbar}{3\pi} \alpha_{\text{fine}} a_H^2 \frac{R_H}{E} \epsilon_{r,\text{opt}} n_r \frac{p_{\text{cv}}^2}{2m} \left(\frac{m_{\text{eff}}}{\hbar^2} \right)^3 \frac{M_C D_{ij}^2}{\rho \omega_{ij} (E_{g0} - E)} \\ &\times \left[f_{\text{BE}}(\omega_{ij}) (E - E_g + \hbar\omega_{ij}) + (f_{\text{BE}}(\omega_{ij}) + 1) (E - E_g - \hbar\omega_{ij}) \right] \end{aligned} \quad (\text{S7})$$

where $\hbar\omega_{ij}$ is energy of a particular phonon mode, E_{g0} is the direct band gap and E_g the indirect band gap, p_{cv} is the momentum matrix element, f_{BE} is the Bose-Einstein distribution, D_{ij} is the deformation potential constant for that phonon mode, ρ is the density of the material, M_C is the number of equivalent conduction band valleys, and $\epsilon_{r,opt} = n_r^2$ is the relative permittivity at optical frequencies. The main differences with respect to the direct transition are therefore the $(E_{g0} - E)^2$ term, the dependence on the deformation potential constant, the different dependence on refractive index and permittivity as well as the quadratic (indirect) vs. the square-root like (direct) dependence of α on $E - E_g$. While the direct absorption coefficient given by Eq. (S1) depends only on readily available parameters like band gap, effective mass and refractive index, equation (S7) for the indirect absorption coefficient is more complex. Therefore, we present a few examples by choosing numbers that correspond to a certain material. We distinguish two cases: (i) is a case, reminiscent of c-Si with rather larger phonon energies and an indirect band gap far above the direct one. If we chose the parameters such as in column Si of table SII, we obtain the pink solid line in Fig. S1. This line is slightly higher than the open symbols representing experimental data for the absorption coefficient of c-Si. If we chose the parameters in the column named MAPI in table SII, we obtain the solid blue line in Fig. S1. Here we assumed that the direct band gap is 100 meV above the indirect band gap. Therefore, we clearly see the singularity caused by the $(E_{g0} - E)^2$ term in Eq. (S7) that is obviously absent in the experimental absorption coefficient of MAPI. For energies above E_{g0} , we just used Eq. (S5) to calculate the direct absorption coefficient. Thus, the solid blue line is a combination of Eq. (S7) for energies below E_{g0} and Eq. (S5) for energies above E_{g0} . While the indirect part of the simulated spectrum is fairly close to the experimental one, the direct part is slightly too optimistic. Thus, Fig. S1 shows that equations derived by Ridley^{1;2} are fairly useful in reproducing the approximate absorption coefficients based on the correct effective masses with the exception

of the singularity produced by Eq. (S7). The $(E_{g_0} - E)^2$ term in Eq. (S7) explains why the indirect part of the absorption coefficient seems to be pretty high in MAPI⁶ but the transition to the direct part of the absorption coefficient requires omitting the values that are within approximately 20 meV of the singularity.

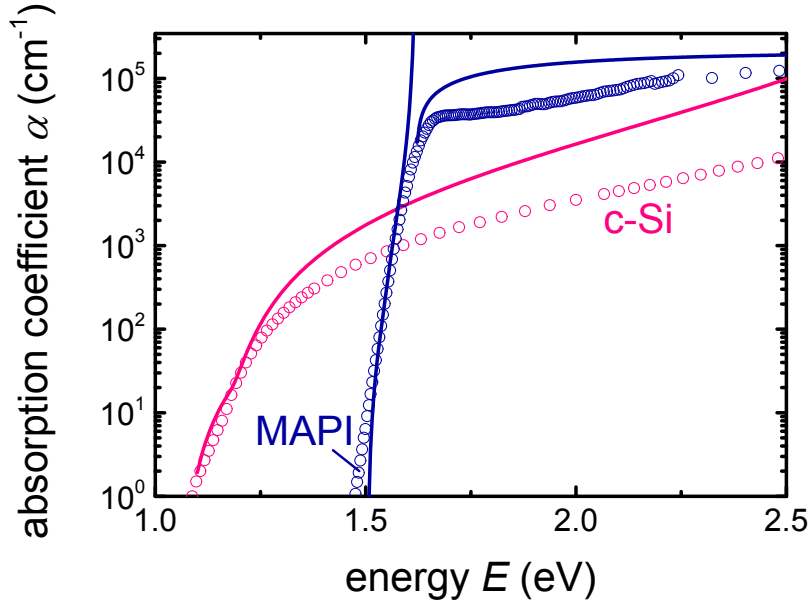


Figure S1: Absorption coefficient as a function of photon energy as obtained when using the parameters in the first two columns of table SII in combination with the equations (S5) and (S7) for the absorption coefficient of direct and indirect semiconductors. In addition, we show the experimental absorption coefficients of crystalline Si (c-Si) and of $\text{CH}_3\text{NH}_3\text{PbI}_3$ (MAPI). In the case of MAPI, we assumed there to be an indirect band gap 100meV below the direct gap, thus, the singularity contained in Eq. (S7) is clearly visible at 1.62 eV. Above that point we used Eq. (S5) for the absorption coefficient of a direct semiconductor.

Table SII: Summary of the parameters needed to calculate the absorption coefficient of direct and indirect semiconductors. The four columns give the parameters chosen for Fig. S1 (column c-Si and MAPI) for comparison with experimental data as well as the two more generic cases used for the main paper.

Parameter	Case c-Si	Case MAPI	Generic indirect	Generic direct
Band gap E_g	1.12 eV	1.52 eV	1.6 eV	1.6 eV
Direct gap E_{g0}	3.2 eV	1.62 eV	5 eV ¹	1.6 eV
Refractive index n_r	3.5	2.5	2.5	2.5
Mass density ρ	2.3 g/cm ³	4.16 g/cm ³	2.3 g/cm ³	-
Momentum matrix element $p_{cv}^2/2m^7$	$\frac{E_g}{4} \left(1 + \frac{m}{m_{\text{eff,V}}}\right)$	$\frac{E_g}{4} \left(1 + \frac{m}{m_{\text{eff}}}\right)$	$\frac{E_g}{4} \left(1 + \frac{m}{m_{\text{eff}}}\right)$	$\frac{E_g}{4} \left(1 + \frac{m}{m_{\text{eff}}}\right)$
Effective mass CB $m_{\text{eff,C}}$	$M_C^{2/3} m_{\text{eff,dos}}$ $= 6^{2/3} 0.32$	0.2 ⁸	variable	variable
Effective mass VB $m_{\text{eff,V}}$	1.1	0.2	variable $= m_{\text{eff,C}}$	variable $= m_{\text{eff,C}}$
Number of equivalent conduction band valleys M_C	6	6	6	-
Deformation potential constant D_{ij} ⁹	5×10^{10} eV/m	5×10^{10} eV/m	5×10^{10} eV/m	-
Optical phonon energy $\hbar\omega_{ij}$	58 meV	16.5 meV ¹⁰	50 meV	-

2. Capture cross section

According to Markvart, the capture cross section for non-radiative transitions via several phonons is given by^{3:4}

$$\sigma \propto \sqrt{\frac{m_{\text{eff}}}{4kT}} \frac{\pi}{\omega \hbar^2} \frac{|V_{nk}|^2}{\sqrt{p\sqrt{1+x^2}}} \exp \left[p \left(\frac{\hbar\omega}{2kT} + \sqrt{1+x^2} - x \cosh \left(\frac{\hbar\omega}{2kT} \right) - \ln \left(\frac{1+\sqrt{1+x^2}}{x} \right) \right) \right], \quad (\text{S8})$$

where the parameter x is related to the number p of phonons involved in the transition and the Huang-Rhys factor S_{HR} via⁵

¹ in order to move the singularity out of the region relevant for photovoltaics

$$x = \begin{cases} \frac{S_{\text{HR}}}{p \sinh(\hbar\omega/2kT)} & \text{for } S_{\text{HR}} < p \\ \frac{p}{S_{\text{HR}} \sinh(\hbar\omega/2kT)} & \text{for } S_{\text{HR}} > p \end{cases} \quad (\text{S9})$$

In Eq. (S8), V_{nk} is the transition matrix element given by Eq. (6.5.8) in ref. ¹¹. The Huang-Rhys factor^{9;12} again depends on phonon energies, on the deformation potential and on the frequency dependent dielectric permittivity. However, it doesn't directly depend on effective mass.

The crucial parameters controlling non-radiative recombination are the SRH lifetimes for electrons and holes. These are related to the capture cross section via

$$\tau_{n,p} = \frac{1}{\sigma_{n,p} v_{\text{th}} N_t} \quad (\text{S10})$$

where v_{th} is the thermal velocity and N_t is the trap density. Noting that $v_{\text{th}} = \sqrt{8kT/\pi m_{\text{eff}}}$,⁴ we conclude that the SHR lifetimes are independent of effective mass.

The capture cross section given by Eq. (S8) is the capture cross section for capture into a neutral defect state. However, capture of electrons or holes into charged defects requires a correction factor called the Sommerfeld factor s . The Sommerfeld factor depends on whether the charges of the charge carrier and the defect have the same or an opposite sign. If the sign of the charge is the same, the defect is repulsive with s given by Eq. (6.5.38) in ref. ¹³. In this situation s is independent of effective mass. In the opposite case, the defect attracts the charge carrier Coulombically and the dimensionless Sommerfeld factor is given by¹³

$$s = 4|Z| \sqrt{\frac{\pi R_{\text{H}} m_{\text{eff}}}{kT m \epsilon_r^2}} \quad (\text{S11})$$

where Z is the ratio between the charge on the defect and the charge of the free carrier (i.e. $Z = \pm 1$ for a singly charged defect). The capture cross section σ_{a} for an attractive defect will then be simply given by $\sigma_{\text{a}} = s\sigma$, using Eq. (S8) for σ and Eq (S11) for s . Thus, a high effective mass will further reduce the smaller of the two lifetimes. In high injection, the longer

lifetime will dominate and therefore this effect will be minor. In low injection, it depends on the doping type and the charge states of the dominant defect, whether this effect will matter or not. In order to keep the discussion generic and simple, we did not include this effect in the simulations in the main paper, but we want to mention it here.

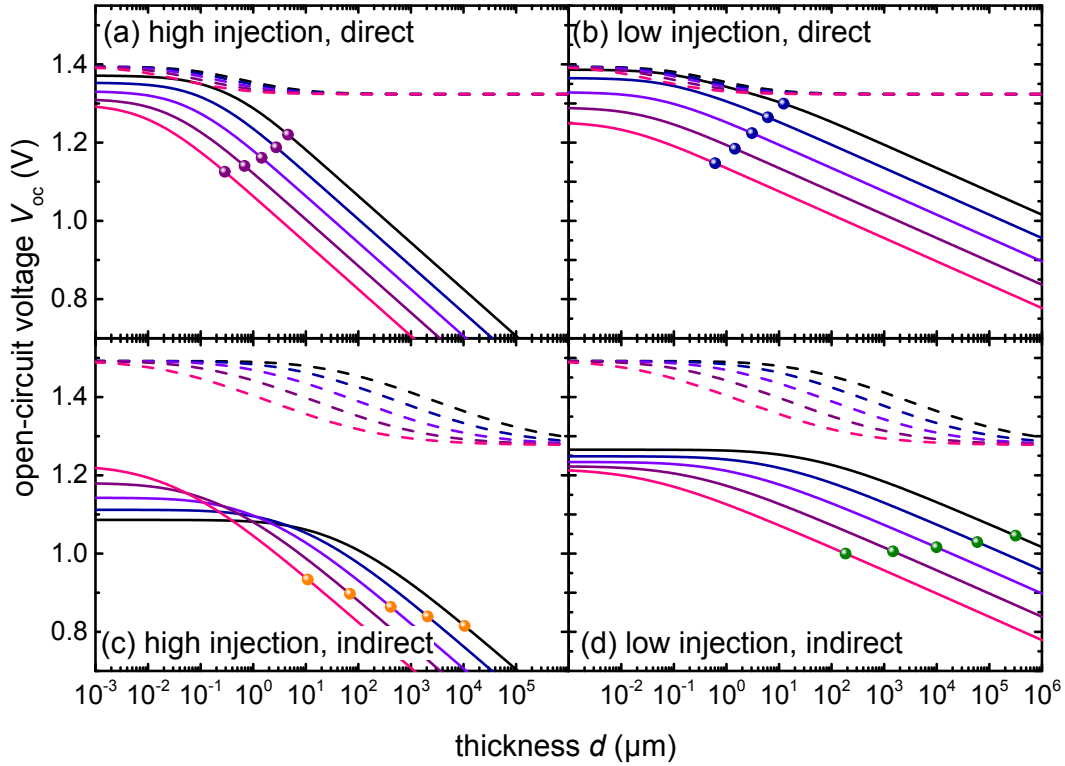


Figure S2: In analogy with Fig. 1 in the main paper, this graph presents the open-circuit voltage V_{OC} as a function of thickness and with the effective density of states as parameter ($N_{\text{eff}} = 10^{18}, 10^{18.5}, 10^{19}, 10^{19.5}, 10^{20} \text{ cm}^{-3}$) for four different cases: The cases are all combinations of high and low level injection (intrinsic and doped semiconductor) and direct and indirect band gap semiconductors. Dashed lines represent the radiative limit and solid lines describe the case with a SRH lifetime $\tau_n = \tau_p = 1 \mu\text{s}$.

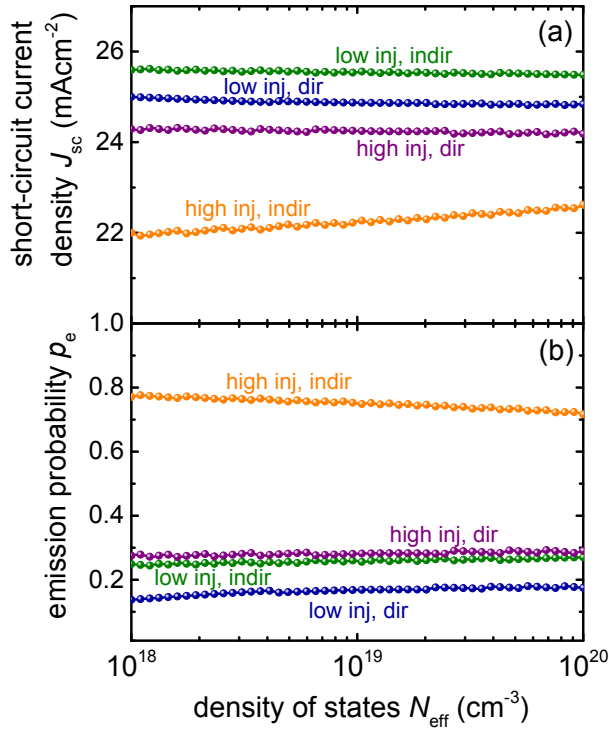


Figure S3: (a) Short-circuit current density J_{sc} and (b) emission probability p_e as a function of effective density of states at the optimum thickness as shown in Fig. 2b in the main paper. Both J_{sc} and p_e are measures of the absorptance of the devices summed up in one parameter. Both do not depend strongly on N_{eff} with the high injection/indirect band gap case being the one with the largest deviation from constant. This implies that the set of equations described in the main paper leads to a rather simple rule of thumb for the optimum thickness. The product of absorption coefficient and optimum thickness remains constant, when N_{eff} or m_{eff} are changed. It does not stay constant when other parameters are varied, which explains why the J_{sc} and p_e values are different comparing the four different scenarios with each other.

Reference List

1. B. K. Ridley, in *Quantum Processes in Semiconductors*, Oxford University Press, Oxford, 2013, pp. 168.
2. B. K. Ridley, in *Quantum Processes in Semiconductors*, Oxford University Press, Oxford, 2013, pp. 186.
3. T. Markvart, *Journal of Physics C: Solid State Physics*, 1981, **14**, L895.
4. T. Markvart, in *Recombination in Semiconductors*, ed.P. T. Landsberg, Cambridge University Press, Cambridge, 2003, pp. 474.
5. T. Markvart, in *Recombination in Semiconductors*, ed.P. T. Landsberg, Cambridge University Press, Cambridge, 2003, pp. 467-468.

6. F. Staub, H. Hempel, J. C. Hebig, J. Mock, U. W. Paetzold, U. Rau, T. Unold, and T. Kirchartz, *Physical Review Applied*, 2016, **6**, 044017.
7. B. K. Ridley, in *Quantum Processes in Semiconductors*, Oxford University Press, Oxford, 2013, pp. 173.
8. Y. Zhou and G. Long, *The Journal of Physical Chemistry C*, 2017, **121**, 1455.
9. B. K. Ridley, in *Quantum Processes in Semiconductors*, Oxford University Press, Oxford, 2013, pp. 224.
10. M. Sendner, P. K. Nayak, D. A. Egger, S. Beck, C. Muller, B. Epding, W. Kowalsky, L. Kronik, H. J. Snaith, A. Pucci, and R. Lovrincic, *Materials Horizons*, 2016, **3**, 613.
11. T. Markvart, in *Recombination in Semiconductors*, ed. P. T. Landsberg, Cambridge University Press, Cambridge, 2003, pp. 470.
12. K. Huang and A. Rhys, *Proceedings of the Royal Society of London. Series A. Mathematical and Physical Sciences*, 1950, **204**, 406.
13. T. Markvart, in *Recombination in Semiconductors*, ed. P. T. Landsberg, Cambridge University Press, Cambridge, 2003, pp. 475.